

Ion bombardment of Fe-based amorphous metallic alloys

Marcel Miglierini · Adriana Lančok · Mária Pavlovič

Published online: 26 March 2009
© Springer Science + Business Media B.V. 2009

Abstract $\text{Fe}_{74}\text{Cu}_1\text{Nb}_3\text{Si}_{16}\text{B}_6$ amorphous metallic alloy is investigated after ion irradiation by 110 keV N^+ and 593 MeV Au ions. The depth-profiles of the radiation damage were calculated by the SRIM2008 code. Applicability of transmission and conversion electron Mössbauer effect measurements to distinguish between the bulk and surface radiation damage is demonstrated by using different irradiation conditions. The investigated alloy is characterized by ferromagnetic interactions. The implantation does not depict appreciable changes of the samples' surfaces. Changes in chemical short-range order (SRO) are revealed in N^+ irradiated alloys. Heavy Au ions caused pronounced effects in the position of the net magnetization though no impact on SRO was observed. After annealing, structural relaxation and annealing-out of the irradiation-induced stresses caused the rotation of the net magnetization back to its original position.

Keywords Ion irradiation · Metallic glasses · Mössbauer spectroscopy · Short-range order · Hyperfine interactions

M. Miglierini (✉) · M. Pavlovič
Department of Nuclear Physics and Technology, Slovak University of Technology,
Bratislava, Slovakia
e-mail: marcel.miglierini@stuba.sk

M. Miglierini
Center for Nanomaterial Research, Palacky University, Olomouc, Czech Republic

A. Lančok
Institute of Physics, AS CR, v. v. i., Prague, Czech Republic

A. Lančok
Institute of Inorganic Chemistry, AS CR, v. v. i., Husinec-Řež, Czech Republic

1 Introduction

Irradiation-induced modifications of amorphous systems attract the interest of many researcher teams for already some time. Thermal neutron irradiation up to a dose of 10^{19} neutrons/cm² has been shown to perturb the short-range order (SRO) of Fe_{78-x}Ni_xSi₈B₁₄ metallic glasses which has lead to an increase of Curie temperature of the Ni-rich alloys [1]. An opposite tendency was observed, however, in Fe₃₀Ni_{48-x}Cr_xMo₂Si₅B₁₅ metallic glass exposed to the whole spectrum of neutron energies [2].

More pronounced changes in magnetic hyperfine interactions were revealed by irradiation of a Fe₉₀Zr₁₀ amorphous alloy with 209 MeV ⁸⁴Kr ions with the fluence of 3×10^{14} ions/cm² [3]. The modification in the magnetic anisotropy introduced by swift heavy-ion irradiation has been investigated in ferromagnetic metallic glasses Fe₇₈B₁₃Si₉ and Fe₄₀Ni₃₈Mo₄B₈ irradiated with 100 MeV ¹²⁷I ions at different fluencies from 5×10^{12} to 7.5×10^{13} ions/cm² [4]. The magnetic anisotropy has been studied by measuring the relative intensity ratio of Mössbauer sextets.

Irradiation with 120 MeV Ag and 350 MeV Au ions of Fe_{0.85}N_{0.15} and Fe_{73.9}Cu_{0.9}Nb_{3.1}Si_{13.2}B_{8.9} amorphous films resulted in gradual removal of anisotropy and a decrease in coercivity, which was attributed to relaxation of internal stresses [5]. This demonstrates that swift heavy-ions can be used for controlled modification of magnetic properties of thin films. At the fluence of 5×10^{13} ions/cm² the in-plane anisotropy completely disappeared.

Among other applications [6], amorphous magnetic metallic alloys are considered for use in accelerator technology to improve performance of RF-cavities. Vacuum cavities would have huge dimensions and it is necessary to reduce their size by filling them with high permeability magnetic materials [7]. However, using such cavities at high-power high-energy accelerators brings an additional problem of exposing the accelerator components to radiation. During the machine operation, the magnetic materials of the cavities are exposed to radiation caused by lost beam particles. Consequently, it is inevitable to study the impact of ion bombardment on structural as well as magnetic characteristics of the construction materials.

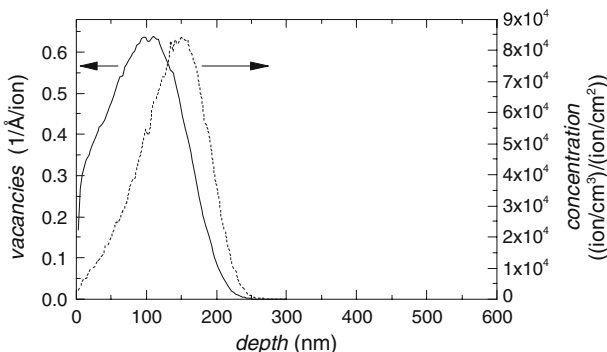
In this contribution we present the study of Fe₇₄Cu₁Nb₃Si₁₆B₆ amorphous metallic alloy irradiated by different ions at different fluencies and energies. As the principal method of investigation we use Mössbauer spectroscopy. This system is a good candidate of an amorphous alloy which is supposed to be used in the FAIR (Facility for Antiproton and Ion Research) accelerator complex [8].

2 Experimental details

Fe₇₄Cu₁Nb₃Si₁₆B₆ soft ferromagnetic alloy was prepared by the method of rapid quenching of a melt in a form of ribbons about 23 μm thick.

The irradiation was performed by 110 keV N⁺ and 593 MeV Au ions to the air side of the ribbons, i.e. the one which was in contact with the surrounding atmosphere during the rapid quenching process of their preparation. The opposite side of the ribbon is denoted as the wheel side. The parameters of the particle beams and their ranges were calculated using the SRIM2008 and S³M codes [9].

Fig. 1 SRIM2008 simulations of radiation damage profile (solid line) and range distribution (dashed line) of 110 keV N⁺ ions implanted into the Fe₇₄Cu₁Nb₃Si₁₆B₆ metallic glass



⁵⁷Fe Mössbauer effect techniques including transmission Mössbauer spectrometry (TMS) and conversion electron MS (CEMS) was applied at room temperature (RT) employing a ⁵⁷Co/Rh radioactive source. TMS provides information about the bulk of the metallic glass whereas the CEMS technique can screen the subsurface regions down to the depth of about 200 nm. Calibration of the apparatus was accomplished by a 12.5 μm thick α-Fe foil at RT. Evaluation of the spectra was done using the Confit fitting software [10].

3 Results and discussion

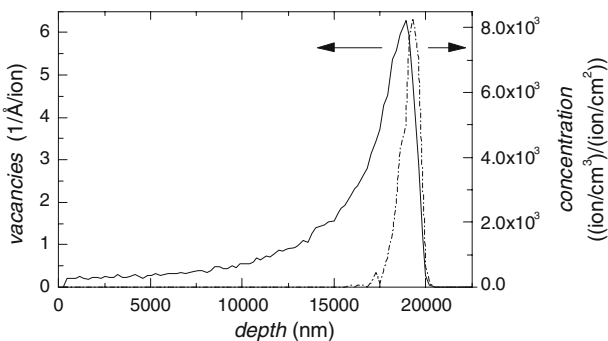
3.1 Simulations of the irradiation experiments

The SRIM simulations were used to find appropriate irradiation energy and to estimate the radiation damage (vacancy production) caused by different ions due to elastic nuclear collisions in the “full cascade” mode [9]. Figure 1 shows the radiation damage profile and the range distribution for 110 keV N⁺ ions implanted into the Finemet-type Fe₇₄Cu₁Nb₃Si₁₆B₆ metallic glass.

The highest number of vacancies produced in the target metallic glass is observed in the depth of about 114 nm where the radiation damage profile (solid line in Fig. 1) attains its maximum. The peak of the ion penetration curve (dashed line), i.e. the depth at which the highest concentration of the stopped ions is found is positioned at about 153 nm, and the mean projected range is 133 nm with the range straggling of 47 nm. Thus, the region of the most severe radiation damage is well correlated to the mean projected range of primary ions and is located at the depth of approximately 133 nm below the sample surface.

Figure 2 shows the same quantities for 593 MeV Au ions. The maxima of the radiation damage profile (solid line in Fig. 2) and the ion penetration range distribution (dashed curve) are located at about 18.9 μm and ca. 19.3 μm, respectively. The mean projected range is 18.9 μm and the range straggling is 575 nm. It should be noted, that while in the case of N⁺ irradiation the region of the most pronounced radiation damage is located within the scanning depth of CEMS (up to 200 nm), here it is buried deep in the bulk of the ribbon-shaped specimen.

Fig. 2 SRIM2008 simulations of radiation damage profile (solid line) and range distribution (dashed line) of 593 MeV Au ions implanted into the Fe₇₄Cu₁Nb₃Si₁₆B₆ metallic glass



3.2 Mössbauer spectrometry

3.2.1 Irradiation with nitrogen

Room temperature ⁵⁷Fe Mössbauer spectra of the Fe₇₄Cu₁Nb₃Si₁₆B₆ metallic glass are characteristic for an amorphous material which shows ferromagnetic interactions. The spectra were evaluated by distributions of magnetic hyperfine fields. No appreciable changes in the shapes of either TMS or CEMS spectra were revealed after N⁺ ion irradiation with respect to the as-quenched (non-irradiated) state of the alloy. This is the reason why we do not show any figure of the measured spectra of the N⁺ irradiated samples. Mössbauer spectrum of the as-quenched alloy will be illustrated in the following section. Taking into consideration the SRIM simulations, this result was expected for the bulk of the irradiated samples. Nevertheless, as the maximum of the radiation damage curve is positioned at about 133 nm some changes were anticipated in the CEMS spectra. This was also not the case and detectable deviations were revealed only in some spectral parameters.

Average values of isomer shifts and hyperfine magnetic fields are plotted against the fluence in Fig. 3. The prediction of non-detectable damage in the bulk of the samples is confirmed by nearly constant isomer shifts and hyperfine fields in the TMS spectra (open squares in Fig. 3). And even though the same holds for hyperfine fields in the surface layers as demonstrated in Fig. 3b by closed circles, notable increase in isomer shift values is observed in Fig. 3a (closed circles) after the irradiation with the fluence of 10¹⁴ N⁺/cm² as derived from CEMS spectra. This indicates that in the most damaged regions localized close to the sample's surface changes in the chemical SRO occur in the amorphous matrix.

We have performed CEMS measurements also at the non-irradiated (wheel) side of the sample irradiated with the highest fluence. No deviations of the respective spectral parameters from those of the as-quenched (non-irradiated) sample are observed as documented by closed diamond in Fig. 3. This result confirms that the opposite side of the ribbon was not affected by the irradiation process at all (for example by an extensive heating-up the sample). As the irradiation was performed in a vacuum, no traces of oxides were identified, either.

As far as the orientation of magnetic moments in the irradiated samples is concerned, the net magnetization exhibits a tendency to move from its original position in the ribbon plane outwards, *i.e.*, perpendicular to the ribbon plane at the air surface of the metallic glass. This is documented in Fig. 4 by decrease of the

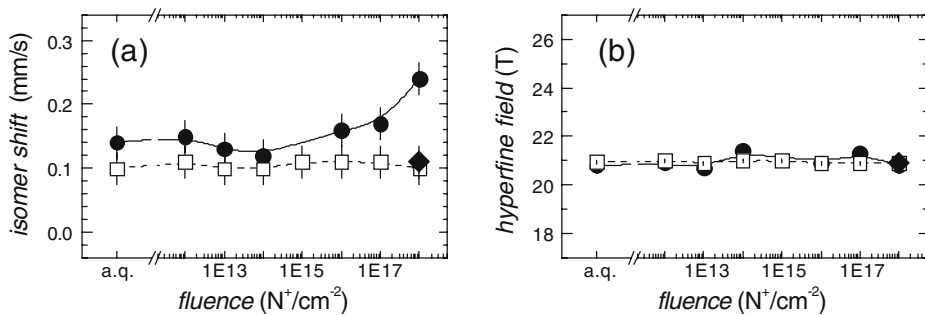
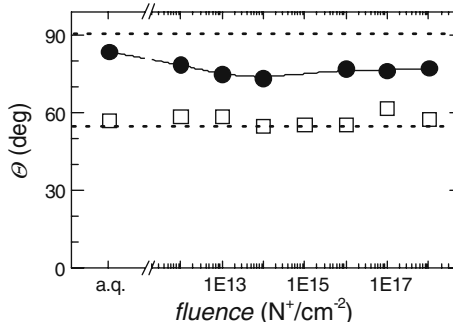


Fig. 3 Average values of isomer shift (**a**) and hyperfine magnetic field (**b**) plotted against the fluence (a.q. as-quenched) as derived from CEMS (closed circle) and TMS (open square) spectra of the $\text{Fe}_{74}\text{Cu}_1\text{Nb}_3\text{Si}_{16}\text{B}_6$ metallic glass irradiated by 110 keV N^+ ions. Parameters derived from CEMS of the non-irradiated surface (closed diamond) are given for comparison

Fig. 4 Angle Θ plotted against the fluence (a.q. as-quenched) as derived from CEMS (closed circle) and TMS (open square) spectra of the $\text{Fe}_{74}\text{Cu}_1\text{Nb}_3\text{Si}_{16}\text{B}_6$ metallic glass irradiated by 110 keV N^+ ions. The dotted lines represent $\Theta = 90^\circ$ and 54.7° , respectively (see text)



Θ -angle. By definition, Θ is an angle between the vector of net magnetization and the propagation direction of the γ -rays in a Mössbauer effect experiment. Because γ -rays are normal to the plane of the absorber (sample), $\Theta = 90^\circ$ (dotted line in Fig. 4) indicates that the magnetization rests in the plane of the sample whereas $\Theta = 0^\circ$ characterizes perpendicular position of the magnetization with respect to the ribbon plane. In case of randomly oriented magnetic moments (e.g., in powder material), $\Theta = 54.7^\circ$ (dotted line in Fig. 4), the so-called magic angle. The information about Θ -angle can be obtained directly from the relative ratio of Mössbauer line intensities.

Again, practically no change in the orientation of the net magnetization is observed for the bulk of the irradiated samples as derived from TMS experiments and the individual magnetic moments are oriented almost randomly ($\Theta \approx 57^\circ$).

4 Irradiation with gold

Selected examples of CEMS and TMS spectra of the $\text{Fe}_{74}\text{Cu}_1\text{Nb}_3\text{Si}_{16}\text{B}_6$ metallic glass before (as-quenched) and after irradiation with 593 MeV Au ions are shown in Fig. 5. As mentioned above, they depict characteristic broad sextuplets of amorphous ferromagnetic alloys.

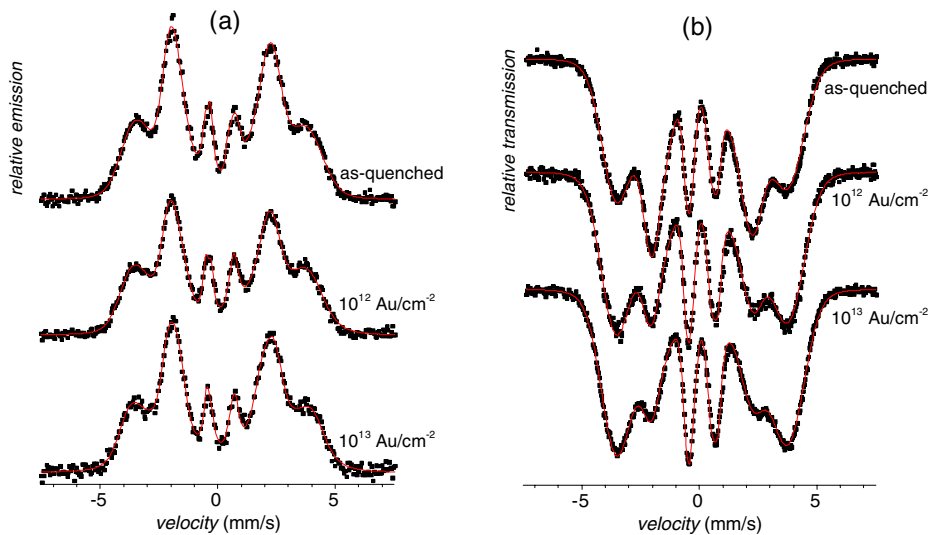


Fig. 5 CEMS (a) and TMS (b) spectra of the $\text{Fe}_{74}\text{Cu}_1\text{Nb}_3\text{Si}_{16}\text{B}_6$ metallic alloy irradiated by 593 MeV Au ions with the indicated fluencies

After irradiation, no appreciable changes are observed in the shapes of the CEMS spectra in Fig. 5a. On the other hand, TMS spectra in Fig. 5b show remarkable decrease in the intensities of the second and fifth lines with rising fluence.

Spectral parameters derived from TMS experiments including isomer shift, hyperfine magnetic field, and Θ -angle are illustrated by opened symbols in Fig. 6 as a function of ion irradiation. As seen from Fig. 6a, the applied ion fluencies had no effect on either isomer shift or hyperfine fields. This means that possible rearrangement of the resonant Fe atoms, i.e. changes in chemical and/or topological SRO are not intensive enough to be reflected by changes of the respective hyperfine parameters. On the other hand, the net magnetization constituted from magnetic moments located in the bulk of the samples turns out of the ribbon plane with rising fluence as demonstrated by opened circles in Fig. 6b. The original close-to-random orientation ($\Theta \approx 56.9^\circ$) is changed by more than 18° .

The repositioning of magnetic moments is caused by internal stresses and magnetostriction of the alloy. The former are introduced during mixing of the atoms (radiation damage) via incident as well as recoil ions during the irradiation. In order to verify this conclusion, we have annealed the irradiated samples for 1 h at 350°C which is far below the onset of crystallization. The resulting TMS spectral parameters are depicted in Fig. 6 by solid symbols.

As seen in Fig. 6a, a moderate increase of isomer shift and hyperfine magnetic field is observed after the annealing. This can be explained by structural relaxation during which the resonant atoms acquire energetically more favourable positions which eventually leads to changes in chemical and also topological SRO. More interesting results are exhibited in Fig. 6b where the structural relaxation has lead to annealing-out of the irradiation-induced stresses. As a consequence, the magnetic moments have acquired positions by about 4.5° closer to the ribbon plane as in the original as-quenched state. It seems that ion irradiation with the fluencies higher than

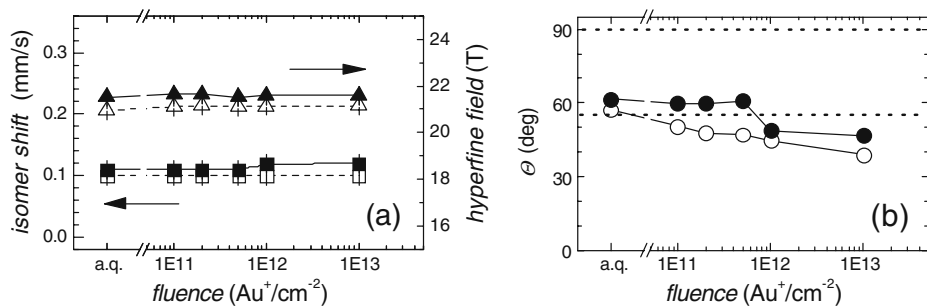


Fig. 6 Average values of isomer shift (squares, left scale) and hyperfine magnetic field (triangles, right scale) (a) and Θ -angle (b) plotted against the fluence (a.q. as-quenched) as derived from TMS spectra of the $\text{Fe}_{74}\text{Cu}_1\text{Nb}_3\text{Si}_{16}\text{B}_6$ metallic glass irradiated by 593 MeV Au ions (open circles) and after annealing at $350^\circ\text{C}/1\text{ h}$ (filled circles)

$5 \times 10^{11} \text{ Au/cm}^{-2}$ caused so high radiation damage which could not be completely removed by the applied annealing conditions. Nevertheless, the magnetization of the samples irradiated with higher fluencies depicts a tendency to rotate back to the ribbon plane.

Changes of the spectral parameters in the CEMS spectra are almost negligible. This result was expected because the radiation damage simulated by the SRIM code has shown minute radiation damage in the subsurface layers (see Fig. 2).

5 Conclusions

Ion irradiation introduces structural rearrangement which can be revealed by Mössbauer spectrometry. Changes in chemical SRO are reflected in isomer shift values whereas topological SRO modifications lead to changes in hyperfine magnetic fields as well as in the orientation of the net magnetization.

The use of rather high fluencies of the N^+ ion irradiation has led to more pronounced changes in the chemical SRO than that of heavier and energetically higher Au ions. Indeed, the observed alternation of the hyperfine spectral parameters depends primarily on the total number of displacements of the resonant atoms which is closely related to the total number of incident ions, i.e. fluence. A systematic study of this phenomenon including simulations is in progress.

Acknowledgements This work was supported by the grants VEGA 1/4011/07, MSM6198959218, EU/INTAS/07, INTAS 06-1000012-8683, AV KAN 400100653, and AVOZ40320502. Samples of Au irradiated metallic glass were supplied by courtesy of Dr. G. Schumacher (Berlin).

References

1. Gupta, A., Habibi, S., Principi, G.: Study of short range order in Fe–Ni–Si–B amorphous alloys. *Mater. Sci. Eng.* **A304–A306**, 1058–1061 (2001)
2. Miglierini, M.: Mössbauer study of neutron irradiated Fe–Ni–Cr–Mo–Si–B metallic glass. *Phys. Rev., B* **44**, 7225–7233 (1991)

3. Kuzmann, E., Lakatos-Varsanyi, M., Nomura, K., Ujihira, Y., Masumoto, T., Principi, G., Tosello, C., Havancsak, K., Vertes, A.: Combination of electrochemical hydrogenation and Mössbauer spectroscopy as a tool to show the radiation effect of energetic heavy-ions in Fe–Zr amorphous alloys. *Electrochem. Commun.* **2**, 130–134 (2000)
4. Amrute, K.V., Nagare, B.J., Fernandes, R.P., Sivakumar, V.V., Gupta, A., Kanjilal, D., Kothari, D.C.: Modification of magnetic anisotropy in ferromagnetic metallic glasses using high energy ion beam irradiation. *Surf. Coat. Technol.* **196**, 135–138 (2005)
5. Dubey, R., Gupta, A., Sharma, P., Darowski, N., Schumacher, G.: Tailoring of magnetic anisotropy in amorphous and nanocrystalline soft magnetic alloys using swift heavy-ions. *J. Magn. Magn. Mater.* **310**, 2491–2493 (2007)
6. McHenry, M.E., Laughlin, D.E.: Nano-scale materials development for future magnetic applications. *Acta. Mater.* **48**, 223–238 (2000)
7. Hofmann, I.: Heavy-ion inertial fusion in Europe. *Nucl. Instr. Methods A* **464**, 24–32 (2001)
8. Spiller, P., Blasche, K., Franczak, B., Kirk, M., Huelsmann, P., Omet, C., Ratschow, S., Stadlmann, J.: Accelerator plans at GSI for plasma physics applications. *Nucl. Instr. Methods A* **544**, 117–124 (2005)
9. Pavlović, M., Strašík, I.: Supporting routines for the SRIM code. *Nucl. Inst. Methods* **B257**, 601–604 (2007)
10. Žák, T., Jirásková, Y.: CONFIT: Mössbauer spectra fitting program. *Surf. Interface Anal.* **38**, 710–714 (2006)